

IL13R α 2 siRNA inhibited cell proliferation, induced cell apoptosis, and suppressed cell invasion in papillary thyroid carcinoma cells

Mingjun Gu

Department of Endocrinology,
Shanghai Gongli Hospital, The Second
Military Medical University, Shanghai,
People's Republic of China

Aim: Papillary thyroid carcinoma (PTC) is the most common type of thyroid cancer. Infiltrative growth and metastasis are the two most intractable characteristics of PTC. Interleukin-13 receptor α 2 (IL13R α 2) with high affinity for Th2-derived cytokine IL-13 has been reported to be overexpressed in several tumors. In this study, an analysis of IL13R α 2 expression in PTC and matched paracancerous tissues was undertaken, and its biologic functions in PTC were assessed.

Methods: IL13R α 2 and vascular endothelial growth factor (VEGF) expression were detected by using real-time polymerase chain reaction and immunohistochemistry analyses. Cell proliferation, invasion, apoptosis, and caspase activity were measured with the Cell Counting Kit-8, Transwell, flow cytometry analyses, and biochemistry assay, respectively.

Results: Upregulation of IL13R α 2 and VEGF was observed in PTC tissues compared with matched paracancerous tissues. Pearson's correlation analysis indicated that IL13R α 2 mRNA level in the tested PTC tissues was positively correlated with VEGF mRNA level. Besides, inhibited cell proliferation, induced cell apoptosis, and suppressed cell invasion were detected in IL13R α 2-silenced PTC-1 cells. Increased activity of Caspase 3 and Caspase 9, along with elevated cleaved Caspase 3 and poly (ADP)-ribose polymerase indicated the signal pathway of cell apoptosis induced by IL13R α 2 siRNA. In addition, downregulated metastasis- and angiogenesis-related proteins VEGF, VEGFR2, MMP2, and MMP9 indicated the decreased number of invading cells after knockdown of IL13R α 2.

Conclusion: The results demonstrate that IL13R α 2 plays an important role in the progress of PTC. IL13R α 2 knockdown in PTC cells inhibited cell proliferation, induced cell apoptosis, and suppressed cell invasion. These data suggest that IL13R α 2 may be a novel therapeutic target in the treatment of PTC clinically.

Keywords: papillary thyroid carcinoma, IL13R α 2 siRNA, metastasis

Introduction

Thyroid cancer is one of the malignancies whose incidence is rapidly increasing in the world, and the incidence rate reached 13.5 per 100,000 in 2008.^{1,2} Papillary thyroid carcinoma (PTC) originating from thyroid epithelial cells is the most frequent type of thyroid cancer, accounting for about 80% of all thyroid cancers.³ Currently, operative treatment and hormone therapy are the main therapies for PTC with favorable prognosis.^{1,4} However, metastasis of PTC to lymphatic vessels remains a severe problem in the clinical treatment of PTC. Previous studies have demonstrated that the clinical outcome of metastatic PTC was affected by several prognostic factors including histologic type, tumor size, tumor infiltration, and vascular or lymphatic

Correspondence: Mingjun Gu
Department of Endocrinology, Shanghai
Gongli Hospital, The Second Military
Medical University, 219 Miaopu Road,
Pudong New Area, Shanghai 200135,
People's Republic of China
Tel +86 21 5885 8730 ext 5224
Email gumj12345@126.com

invasion, among which genetic factors were found to be the main reason for the development of PTC.⁴

Interleukin-13 receptor $\alpha 2$ (IL13R $\alpha 2$) has high affinity to Th2-derived cytokine IL-13. Because of the short cytoplasmic domain, IL13R $\alpha 2$ has previously been regarded as a decoy receptor to inhibit IL-13-mediated JAK–STAT6 activation.⁵ Subsequent research suggests that binding of IL13R $\alpha 2$ to IL-13 induces TGF- $\beta 1$ through the AP-1 complex.⁶ The elevated expression of IL13R $\alpha 2$ has been observed in several human tumors, such as in prostate, kidney, and pancreatic cancer.^{7–12} IL13R $\alpha 2$ is shown to promote the invasion and metastasis of pancreatic, colon, ovarian, and breast cancer.^{8,13–15} Patients with benign or malignant thyroid disease had significantly higher serum levels of IL-13 as compared to healthy controls.¹⁶ Vascular endothelial growth factor (VEGF) is overexpressed in PTC, and its expression is associated with the incidence of metastasis.¹⁷ VEGF is stimulated by IL-13 and then mediates the protective effects of IL-13 on hyperoxic acute lung injury.¹⁸ However, there are no studies comparing the expression of IL13R $\alpha 2$ between PTC tissues and paracancerous tissues, as well as investigating the contribution of IL13R $\alpha 2$ to papillary thyroid carcinogenesis. In addition, the association between VEGF and IL13R $\alpha 2$ in PTC has not been documented.

In the present study, expression levels of IL13R $\alpha 2$ and VEGF in PTC tissues and paracancerous tissues were measured. Besides, cell proliferation, apoptosis rate, and invasion ability were evaluated in two PTC cell lines after IL13R $\alpha 2$ knockdown. Furthermore, Western blot was employed to measure the signaling pathway proteins. The results suggest that IL13R $\alpha 2$ may function as an oncogene during papillary thyroid carcinogenesis.

Materials and methods

Tissue samples

The study protocol was approved by the local independent ethical committee of Shanghai Gongli Hospital (IE14013, date: September 4, 2014) and was performed according to the ethics committee's guidelines. PTC tissue samples and paired paracancerous tissues were obtained from 45 patients after all the participants had given written informed consent.

Real-time polymerase chain reaction (PCR) analysis

Total RNA was isolated from tissue samples or cultured cell lines by using Trizol Reagent (Invitrogen; Thermo Fisher Scientific). cDNA was synthesized by using a reverse transcription kit (Fermentas, Shanghai, People's Republic of

China) and Oligo(dt)₁₈. Then real-time PCR was conducted by using SYBR Green PCR kit (Thermo Fisher Scientific, Waltham, MA, USA) on the ABI 7300 Real-Time PCR System (Applied Biosystems, Waltham, MA, USA) with the following primers: IL13R $\alpha 2$, 5' GCATTGAAGCGAAGATACAC 3' and 5' ACGCAATCCATATCCTGAAC 3'; VEGF, 5' ATTTCTGGGATTCCTGTAG 3' and 5' CAGTGAAGACACCAATAAC 3'; glyceraldehyde-3-phosphate dehydrogenase (GAPDH), 5' CACCCACTCCTCCACCTTTG 3' and 5' CCACCACCCTGTTGCTGTAG 3'. The PCR conditions were as follows: 10 minutes at 95°C, and then 40 cycles of 15 seconds at 95°C, and 45 seconds at 60°C. Data were collected and analyzed using ABI Prism 7300 SDS Software (Applied Biosystems; Thermo Fisher Scientific).

Immunohistochemistry analysis

After fixation in 10% formalin for 48 hours, the tissue samples were processed with histological embedding techniques and cut into 4 μ m-thick sections. The slides were deparaffinized in xylene and rehydrated in graded alcohols. For antigen retrieval, the sections were autoclaved using a high-pressure method for 15 minutes in a commercially available 0.01 M sodium citrate solution (pH 6.0). Subsequently, the slides were incubated with 3% hydrogen peroxide in phosphate-buffered saline (PBS, pH 7.4) for 10 minutes to quench endogenous peroxidases. Slides were then probed with the primary antibody against IL13R $\alpha 2$ (Abcam, Cambridge, UK) or VEGF (Abcam) for 1 hour at room temperature, followed by horseradish peroxidase-labeled secondary antibody for another 30 minutes at room temperature. After the antibody–antigen reaction, chromogen diaminobenzidine was applied to the slides. Finally, the sections were counterstained with 10% Harris hematoxylin, dehydrated, and mounted.

Cell culture and transfection

PTC cell lines, TPC-1 and ARO, were obtained from the Chinese Academy of Sciences (Shanghai, People's Republic of China) and cultured in Dulbecco's Minimum Essential Medium (DMEM) containing 10% fetal calf serum (FCS) and antibiotics in a humidified atmosphere with 5% CO₂ at 37°C. Cells were digested with trypsin and seeded into a six-well plate (5 \times 10⁵ cells/well) before transfection. Lipofectamine™ 2000 (Invitrogen) was used to transfect IL13R $\alpha 2$ siRNAs (siRNA-1, GGCUAUCGGAUGCUUAUUAU); siRNA-2 (CAGGAUAUGGAUUGCGUAU) or negative control siRNA (NC) into PTC cells. At 48 hours posttransfection, cells were collected and evaluated for knockdown effect by using real-time PCR and Western blot assay. Then,

transfected TPC-1 and ARO cells were processed for Cell Counting Kit-8 (CCK-8), flow cytometry, Transwell, biochemistry, Western blot, and real-time PCR analyses.

Western blot assay

Western blot assay was employed to determine the IL13R α 2 and related proteins' expression level in PTC cell lines. Cells were washed twice with ice-cold PBS followed by incubation with the RIPA lysis buffer (Beyotime, Haimen, People's Republic of China) at 4°C. The extracted protein was collected by centrifugation at 12,000 rpm for 15 minutes at 4°C. Protein concentrations were determined by using bicinchoninic acid method (Thermo Fisher Scientific). Equal amounts of protein from each sample were loaded on 10% sodium dodecylsulphate–polyacrylamide gels. After electrophoresis, proteins on the gel were transferred onto a nitrocellulose blotting membrane (Millipore, Billerica, MA, USA) and incubated with 5% skim milk in Tris-buffered saline Tween 20 at 4°C for 1 hour. The membranes were then incubated with antibodies against IL13R α 2 (Abcam), VEGF (Abcam), VEGFR2 (Affinity, Cincinnati, OH, USA), MMP2 (Abcam), MMP9 (Abcam), cleaved Caspase 3 (Abcam), cleaved poly (ADP)-ribose polymerase (PARP), or GAPDH (Cell Signaling Technology, Danvers, MA, USA) for 2 hours at room temperature. Then the membrane was washed three times with Tris-buffered saline and incubated with horseradish peroxidase-conjugated secondary antibodies (Beyotime) for 1 hour. Immunoreactive bands were detected using an ECL detection kit (Millipore). The densities of the bands were semi-quantified using ImageJ software.

CCK-8 assay

Cultured PTC cells were trypsinized, plated into 96-well plates (2×10^3 cells/well), and incubated at 37°C overnight. The cells were then transfected with siRNA-1, siRNA-2, or NC. At 0, 24, 48, and 72 hours posttransfection, 100 μ L DMEM containing 10% CCK-8 (Dojindo Biochem., Kumamoto, Japan) was added to each well, and then incubated in 5% CO₂ at 37°C for 1 hour. The OD_{450 nm} was measured using a spectrophotometer to evaluate cell proliferation.

Flow cytometry

At 48 hours after transfection, cells were collected, washed with PBS, and centrifuged at 1,000 rpm for 5 minutes. The pelleted cells were then labeled with Annexin V fluorescein isothiocyanate apoptosis detection kit (BD Biosciences, Franklin Lakes, NJ, USA) at room temperature for 20 minutes in the dark. Cell apoptosis rate was evaluated using a flow cytometer (FACS Calibur, BD Biosciences).

Transwell analysis

Transfected cells were starved in serum-free DMEM overnight, trypsinized, and diluted to 3×10^5 cells/mL in DMEM containing 1% FCS. Cell suspension at a volume of 0.3 mL was added into the upper chamber precoated with matrigel, and 0.75 mL DMEM containing 10% FCS was added into the lower chamber. After the incubation for 48 hours, the cells remaining in the upper surface were carefully removed. The invaded cells were fixed by formalin for 10 minutes, stained with 0.5% crystal violet for 30 minutes, and counted in three randomly selected visual fields under a microscope (OLYMPUS, Shenzhen, People's Republic of China) at $\times 200$ magnification.

Biochemical test

The activities of Caspase 3 and Caspase 9 were assessed using Caspase 3 and Caspase 9 colorimetric assay kits (Keygen Biotech Ltd., Nanjing, People's Republic of China) following the manufacturer's protocols. Cultured and transfected cells were collected and washed twice with PBS, followed by lysis with 100 μ L precooled lysis buffer. The supernatant was collected by centrifugation at 10,000 rpm for 1 minute. Protein concentrations were determined using the bicinchoninic acid method. An equal volume of supernatant and $2 \times$ reaction buffer were mixed in a tube, and 5 μ L of Caspase 3 or Caspase 9 substrate was added. After 4 hours of incubation at 37°C, the activity of Caspase 3 and Caspase 9 was measured at OD_{400 nm}.

Statistical analysis

GraphPad Prism software (GraphPad Software, Inc., La Jolla, CA, USA) was used for data analysis. Student's *t*-test was used to analyze the differences of IL13R α 2 and VEGF expression between PTC and paracancerous tissues. Pearson's correlation test was applied to determine the existence of a relation between IL13R α 2 and VEGF expression in PTC tissues. One-way analysis of variance followed by Tukey's post hoc test was performed for multiple comparison. A *P*-value < 0.05 was defined as statistically significant.

Results

Higher expression levels of IL13R α 2 and VEGF were detected in PTC tissues

Real-time PCR was employed to evaluate the IL13R α 2 and VEGF expression in 45 pairs of PTC tissues and paracancerous tissues. As the results illustrate in Figure 1A and B, higher mRNA levels of IL13R α 2 and VEGF were measured in PTC tissues in comparison to those in paracancerous tissues, with significant differences ($P < 0.01$), indicating the overexpression of IL13R α 2 and VEGF in PTC tissues.

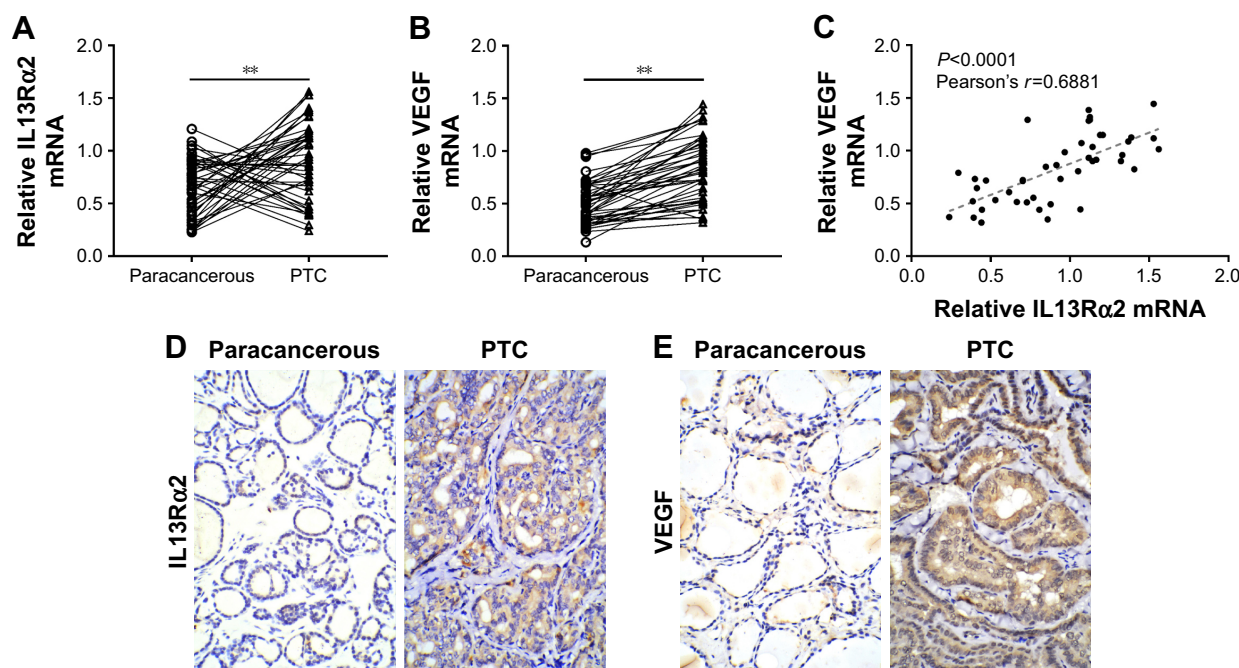


Figure 1 Higher expression level of IL13R α 2 and VEGF were detected in PTC tissues.

Notes: Higher mRNA levels of IL13R α 2 (**A**) and VEGF (**B**) were measured in PTC tissue samples ($n=45$) by using real-time PCR compared with paracancerous tissues ($n=45$). $**P<0.01$, compared with paracancerous tissues. (**C**) Pearson's correlation analysis between IL13R α 2 and VEGF mRNA expression in PTC tissues ($n=45$). Protein levels of IL13R α 2 (**D**) and VEGF (**E**) in PTC and paracancerous tissues were evaluated by using immunohistochemistry analysis. Smaller staining areas of IL13R α 2 and VEGF were observed in paracancerous tissues, indicating the overexpression of IL13R α 2 and VEGF in PTC tissues.

Abbreviations: IL13R α 2, interleukin-13 receptor α 2; PCR, polymerase chain reaction; PTC, papillary thyroid carcinoma; VEGF, vascular endothelial growth factor.

In addition, Pearson's correlation analysis indicated that IL13R α 2 mRNA level in the tested PTC tissues was significantly positively correlated with VEGF mRNA level ($P<0.0001$) (Figure 1C). Subsequently, immunohistochemistry analysis was performed, and higher protein levels of IL13R α 2 and VEGF were also observed in PTC tissues compared with paracancerous tissues (Figure 1D and E).

Knockdown of IL13R α 2 inhibited cell proliferation in PTC cells

To further investigate the role of IL13R α 2 in PTC, we knocked down IL13R α 2 through siRNA transfection. In order to identify the interference effect, the expression of IL13R α 2 in PTC cell lines, TPC-1 and ARO, transfected with IL13R α 2 siRNAs (siRNA-1 or siRNA-2) was measured through Western blot and real-time analyses. As shown in Figure 2A and B, siRNA-transfected PTC cells exhibited significantly decreased mRNA and protein expression of IL13R α 2 compared with NC-transfected cells and control cells ($P<0.001$), indicating the efficient gene silencing of IL13R α 2 siRNAs. Subsequently, cell proliferation of TPC-1 and ARO cells with IL13R α 2 silenced was evaluated by using CCK-8. As shown in Figure 2C, cell proliferation of PTC cells as detected by using CCK-8 was significantly reduced at 24, 48, and 72 hours after the treatment with

IL13R α 2 siRNAs in comparison to NC group and control group, indicating the inhibition effect of IL13R α 2 siRNAs on cell proliferation of PTC cells.

IL13R α 2 siRNA induced cell apoptosis

Annexin V/propidium iodide staining followed by flow cytometry analysis was then applied to detect cell apoptosis. The lower right quadrant of the histograms presents the early apoptotic cells. Figure 3A shows a significantly induced cell apoptosis in IL13R α 2 siRNA groups (siRNA-1 and siRNA-2) in comparison to NC group and control group ($P<0.001$). Further, the activity of proapoptotic proteins Caspase 3 and Caspase 9 measured by using biochemical analysis demonstrated upregulation after the treatment with IL13R α 2 siRNA (Figure 3B). The expression of cleaved Caspase 3 and PARP was upregulated in IL13R α 2 siRNA groups (siRNA-1 and siRNA-2) as compared to control groups (Figure 3C). These findings further indicated the proapoptotic ability of IL13R α 2 siRNA.

IL13R α 2 siRNA inhibited cell invasion

Besides, Transwell assay was performed to evaluate the invasive capacity of TPC-1 and ARO cells. As the result shows in Figure 4A, the invasion capacity of TPC-1 cells treated with IL13R α 2 siRNAs (siRNA-1 and siRNA-2) was

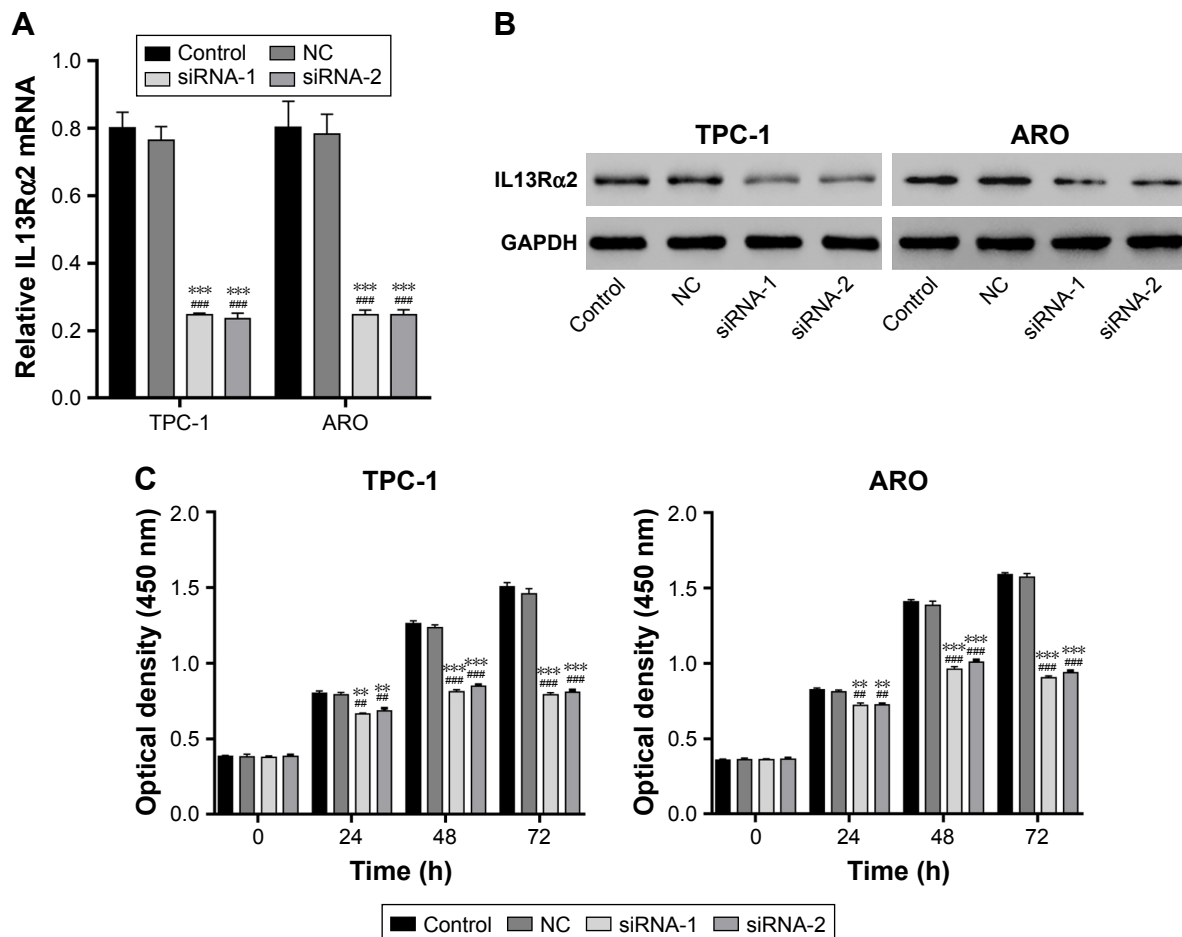


Figure 2 Knockdown of IL13R α 2 inhibited cell proliferation.

Notes: (A) The mRNA expression level of IL13R α 2 was measured by using real-time PCR in TPC-1 and ARO cells with IL13R α 2 siRNA transfection (siRNA-1 or siRNA-2). (B) The IL13R α 2 protein expression was measured by Western blot in TPC-1 and ARO cells after the transfection with IL13R α 2 siRNAs (siRNA-1 and siRNA-2). (C) IL13R α 2 siRNA inhibited cell proliferation in TPC-1 and ARO cells. ** P <0.01, *** P <0.001, compared with the NC group. # P <0.01, ### P <0.001, compared with the NC group (n =3).

Abbreviations: IL13R α 2, interleukin-13 receptor α 2; NC, negative control siRNA; PCR, polymerase chain reaction.

suppressed dramatically compared with the NC and control group (P <0.001).

Knockdown of IL13R α 2 changed the expression of metastasis- and angiogenesis-related proteins

To further investigate the possible mechanisms involved in the functions of IL13R α 2 siRNA, the expression levels of VEGF, VEGFR2, MMP2, and MMP9 in TPC-1 and ARO cells were measured by Western blot. Compared with control group, expression levels of VEGF, VEGFR2, MMP2, and MMP9 exhibited downregulation with a significant difference in PTC cells transfected with IL13R α 2 siRNA (Figure 4B, P <0.001).

Discussion

In the present study, the overexpression of IL13R α 2 in PTC was demonstrated, which has been reported in other

malignancies,⁷⁻¹¹ and the overexpression of VEGF in PTC tissues was confirmed. Additionally, a positive correlation between IL13R α 2 and VEGF expression was observed in PTC tissues. Further, the possible role of IL13R α 2 in the progress of PTC was investigated through knockdown of the receptor. As the results obtained in this study show, inhibited cell proliferation, induced cell apoptosis rate, and suppressed cell invasion in IL13R α 2 silenced cells suggest that IL13R α 2 may function as an oncogene in PTC.

Consistent with the previous report that IL13R α 2 knockdown could induce apoptosis of glioma cells,¹⁹ the results of flow cytometry analysis showed a significant increase in apoptosis rate of TPC-1 and ARO cells after the treatment with IL13R α 2 siRNA. Caspases are critical mediators of cell apoptosis. During programmed cell death, Caspase 9, an initial Caspase, is activated and then activates downstream Caspases, such as Caspase 3 and Caspase 7.²⁰ Activated Caspase 3 induces the cleavage of downstream substrates,

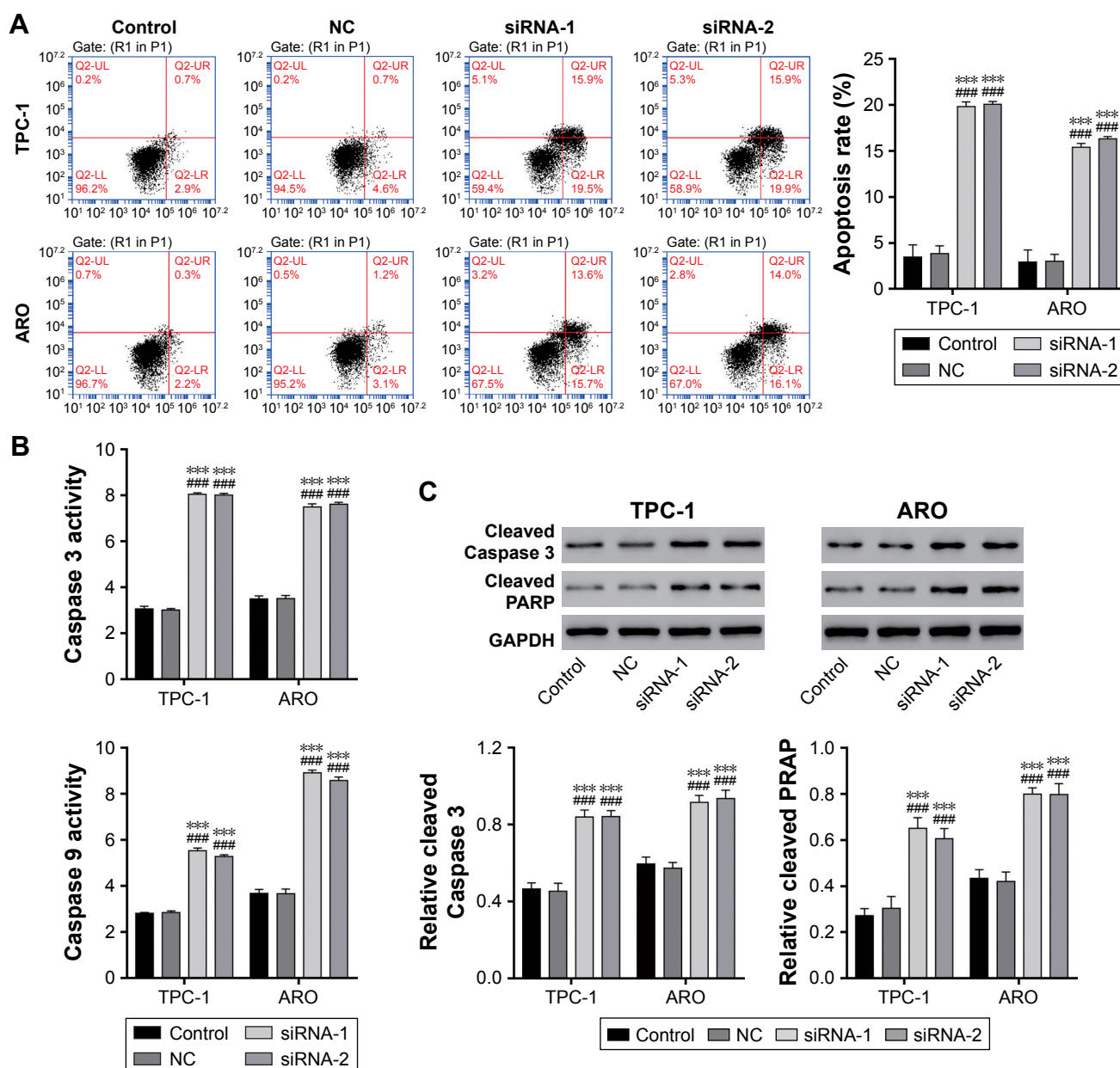


Figure 3 Knockdown of IL13R α 2 induced cell apoptosis in PTC cells.

Notes: (A) TPC-1 and ARO cells with IL13R α 2 knocked down showed a significant increase in apoptosis rate. (B) Increased activity of Caspase 3 and Caspase 9 were detected in TPC-1 and ARO cells after the knockdown of IL13R α 2. (C) The expression of cleaved Caspase 3 and PARP was determined by Western blot. *** P <0.001, compared with the NC group. **** P <0.001, compared with the NC group (n =3).

Abbreviations: GAPDH, glyceraldehyde-3-phosphate dehydrogenase; IL13R α 2, interleukin-13 receptor α 2; NC, negative control siRNA; PARP, poly (ADP)-ribose polymerase; PTC, papillary thyroid carcinoma.

including PARP,²¹ and the release of Caspase-activated deoxyribonuclease, leading to the prevention of DNA repair cycles, the degradation of DNA, instability of chromatin, and ultimately the apoptosis of cells.^{22–24} Here, upregulated Caspase 3 and Caspase 9 activity and elevated cleavage of Caspase 3 and PARP were detected in PTC cells with IL13R α 2 silenced. Our study demonstrated that the increased apoptosis caused by depletion of IL13R α 2 was involved in the upregulated activity of Caspase 3.

Infiltrative growth and metastasis are the two most intractable characteristics of PTC that contribute to the poor prognosis of PTC.^{2–4} Consistent with the previous report in glioma cells,²⁵ our results showed a significant reduction in the growth and invasion of TPC-1 and ARO cells after the treatment with IL13R α 2 siRNA. Epithelial–mesenchymal transition and mesenchymal–epithelial transition are essential for tumor metastasis. The basement membrane is mostly composed of Type IV collagen which is degraded by MMP

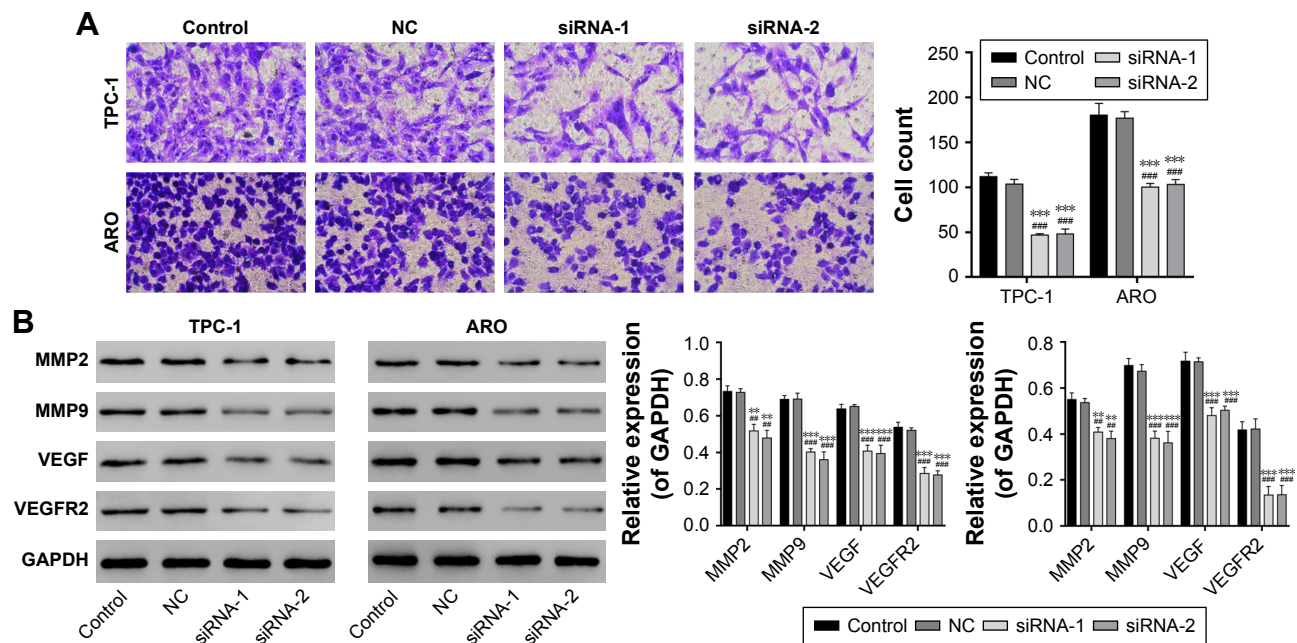


Figure 4 IL13R α 2 siRNA inhibited cell invasion in TPC-1 cells.

Notes: (A) Downregulation of invasion rate was detected in TPC-1 and ARO cells after the transfection with IL13R α 2 siRNAs (siRNA-1 and siRNA-2). (B) Expression levels of VEGF, VEGFR2, MMP2, and MMP9 in TPC-1 and ARO cells were measured by using Western blot analysis. ** $P < 0.01$, *** $P < 0.001$, compared with the NC group. ### $P < 0.01$, #### $P < 0.001$, compared with the NC group ($n = 3$).

Abbreviations: GAPDH, glyceraldehyde-3-phosphate dehydrogenase; IL13R α 2, interleukin-13 receptor α 2; MMP2, matrix metalloproteinase 2; MMP9, matrix metalloproteinase 9; NC, negative control siRNA; VEGF, vascular endothelial growth factor; VEGFR2, VEGF receptor 2.

family proteins MMP2 and MMP9. The basement membrane maintains tissue organization, provides structural support to the cells, and influences cell signaling and polarity.²⁶ Mesenchymal–epithelial transition accompanied by the degradation of basement membrane promotes epithelial–mesenchymal transition, which is an essential step for the metastatic progression in most cancers.²⁷ Besides, tumor angiogenesis factors involved in generation of tumor blood vessels play a crucial role in tumor metastasis, resulting in the uncontrolled growth of tumor. Angiogenesis during mesenchymal–epithelial transition is a complicated process regulated by several positive and negative regulatory factors.^{28,29} It has been demonstrated that VEGF as a specific heparin-binding growth factor in vascular endothelial cells can induce angiogenesis through the recruitment of tumor-associated macrophages, which participate actively in the angiogenesis and growth of tumors.³⁰ In this study, the number of invading cells declined significantly after the knockdown of IL13R α 2 in comparison to NC, suggesting that IL13R α 2 is involved in the invasion of PTC cells. Correspondingly, downregulation of MMP2, MMP9, VEGF, and VEGFR2 was observed in PTC cells after transfection with IL13R α 2 siRNA. All these findings suggested the inhibition ability of IL13R α 2 siRNA in tumor metastasis of PTC.

Conclusion

Overall, it was demonstrated that IL13R α 2 and VEGF are upregulated in PTC. IL13R α 2 knockdown in PTC cells resulted in inhibited cell proliferation, induced cell apoptosis, and suppressed cell invasion. IL13R α 2 knockdown also suppressed the activity of Caspase 3 and Caspase 9, and reduced the expression of VEGF, VEGFR2, MMP2, and MMP9. Thus, these results suggest that IL13R α 2 may be a novel therapeutic target in the treatment of PTC, clinically.

Acknowledgment

This study was supported by the Shanghai Health and Family Planning Commission (number 201440050), Shanghai Science and Technology Committee (number 15ZR1437100), and the Medical Technology Innovative Program of Nanjing Military Region of China (number 2011MA034).

Disclosure

The author reports no conflicts of interest in this work.

References

1. Lam AK, Lo CY, Lam KS. Papillary carcinoma of thyroid: a 30-yr clinicopathological review of the histological variants. *Endocr Pathol*. 2005;16(4):323–330.

2. Yu XM, Schneider DF, Levenson G, Chen H, Sippel RS. Follicular variant of papillary thyroid carcinoma is a unique clinical entity: a population-based study of 10,740 cases. *Thyroid*. 2013;23(10):1263–1268.
3. Lang BH, Lo CY, Chan WF, Lam AK, Wan KY. Classical and follicular variant of papillary thyroid carcinoma: a comparative study on clinicopathologic features and long-term outcome. *World J Surg*. 2006;30(5):752–758.
4. Sebastian SO, Gonzalez JR, Paricio PP, et al. Papillary thyroid carcinoma: prognostic index for survival including the histological variety. *Arch Surg*. 2000;135(3):272–277.
5. Rahaman SO, Sharma P, Harbor PC, Aman MJ, Vogelbaum MA, Haque SJ. IL-13R α 2, a decoy receptor for IL-13 acts as an inhibitor of IL-4-dependent signal transduction in glioblastoma cells. *Cancer Res*. 2002;62(4):1103–1109.
6. Fichtner-Feigl S, Strober W, Kawakami K, Puri RK, Kitani A. IL-13 signaling through the IL-13 α 2 receptor is involved in induction of TGF- β 1 production and fibrosis. *Nat Med*. 2006;12(1):99–106.
7. Bernard J, Treton D, Vermot-Desroches C, et al. Expression of interleukin 13 receptor in glioma and renal cell carcinoma: IL13R α 2 as a decoy receptor for IL13. *Lab Invest*. 2001;81(9):1223–1231.
8. Fujisawa T, Joshi B, Nakajima A, Puri RK. A novel role of interleukin-13 receptor alpha2 in pancreatic cancer invasion and metastasis. *Cancer Res*. 2009;69(22):8678–8685.
9. He H, Xu J, Nelson PS, et al. Differential expression of the alpha2 chain of the interleukin-13 receptor in metastatic human prostate cancer ARCaPM cells. *Prostate*. 2010;70(9):993–1001.
10. Jain M, Zhang L, He M, et al. Interleukin-13 receptor alpha2 is a novel therapeutic target for human adrenocortical carcinoma. *Cancer*. 2012;118(22):5698–5708.
11. Kawakami M, Kawakami K, Kasperbauer JL, et al. Interleukin-13 receptor α 2 chain in human head and neck cancer serves as a unique diagnostic marker. *Clin Cancer Res*. 2003;9(17):6381–6388.
12. Wanibuchi M, Kataoka-Sasaki Y, Sasaki M, et al. Interleukin-13 receptor alpha 2 as a marker of poorer prognosis in high-grade astrocytomas. *J Neurosurg Sci*. Epub 2017 Jan 12.
13. Fujisawa T, Joshi BH, Puri RK. IL-13 regulates cancer invasion and metastasis through IL-13R α 2 via ERK/AP-1 pathway in mouse model of human ovarian cancer. *Int J Cancer*. 2012;131(2):344–356.
14. Barderas R, Bartolome RA, Fernandez-Acenero MJ, Torres S, Casal JI. High expression of IL-13 receptor alpha2 in colorectal cancer is associated with invasion, liver metastasis, and poor prognosis. *Cancer Res*. 2012;72(11):2780–2790.
15. Papageorgis P, Ozturk S, Lambert AW, et al. Targeting IL13Ralpha2 activates STAT6-TP63 pathway to suppress breast cancer lung metastasis. *Breast Cancer Res*. 2015;17(1):98.
16. Provatopoulou X, Georgiadou D, Sergentanis TN, et al. Interleukins as markers of inflammation in malignant and benign thyroid disease. *Inflamm Res*. 2014;63(8):667.
17. Lennard CM, Patel A, Wilson J, et al. Intensity of vascular endothelial growth factor expression is associated with increased risk of recurrence and decreased disease-free survival in papillary thyroid cancer. *Surgery*. 2001;129(5):552–558.
18. Corne J, Chupp G, Lee CG, et al. IL-13 stimulates vascular endothelial cell growth factor and protects against hyperoxic acute lung injury. *J Clin Invest*. 2000;106(6):783.
19. Shi J, Hou S, Huang J, et al. An MSN-PEG-IP drug delivery system and IL13Ralpha2 as targeted therapy for glioma. *Nanoscale*. 2017;9(26):8970–8981.
20. Hengartner MO. The biochemistry of apoptosis. *Nature*. 2000;407(6805):770–776.
21. Nicholson DW, Ali A, Thornberry NA, et al. Identification and inhibition of the ICE/CED-3 protease necessary for mammalian apoptosis. *Nature*. 1995;376(6535):37–43.
22. Debatin KM. Apoptosis pathways in cancer and cancer therapy. *Cancer Immunol Immunother*. 2004;53(3):153–159.
23. Stennicke HR, Salvesen GS. Biochemical characteristics of caspases-3, -6, -7, and -8. *J Biol Chem*. 1997;272(41):25719–25723.
24. Decker P, Isenberg D, Muller S. Inhibition of caspase-3-mediated poly (ADP-ribose) polymerase (PARP) apoptotic cleavage by human PARP autoantibodies and effect on cells undergoing apoptosis. *J Biol Chem*. 2000;275(12):9043–9046.
25. Tu M, Wang W, Cai L, Zhu P, Gao Z, Zheng W. IL-13 receptor α 2 stimulates human glioma cell growth and metastasis through the Src/PI3K/Akt/mTOR signaling pathway. *Tumor Biol*. 2016;37(11):14701–14709.
26. Tetlow LC, Adlam DJ, Woolley DE. Matrix metalloproteinase and proinflammatory cytokine production by chondrocytes of human osteoarthritic cartilage: associations with degenerative changes. *Arthritis Rheum*. 2001;44(3):585–594.
27. Waerner T, Alacakaptan M, Tamir I, et al. ILEI: a cytokine essential for EMT, tumor formation, and late events in metastasis in epithelial cells. *Cancer Cell*. 2006;10(3):227–239.
28. Nyberg P, Salo T, Kalluri R. Tumor microenvironment and angiogenesis. *Front Biosci*. 2008;13(7):6537–6553.
29. Yu Z, Lu B, Sheng Y, Zhou L, Ji L, Wang Z. Andrographolide ameliorates diabetic retinopathy by inhibiting retinal angiogenesis and inflammation. *Biochim Biophys Acta*. 2015;1850(4):824–831.
30. Bailey C, Negus R, Morris A, et al. Chemokine expression is associated with the accumulation of tumour associated macrophages (TAMs) and progression in human colorectal cancer. *Clin Exp Metastasis*. 2007;24(2):121–130.

OncoTargets and Therapy

Publish your work in this journal

OncoTargets and Therapy is an international, peer-reviewed, open access journal focusing on the pathological basis of all cancers, potential targets for therapy and treatment protocols employed to improve the management of cancer patients. The journal also focuses on the impact of management programs and new therapeutic agents and protocols on

Submit your manuscript here: <http://www.dovepress.com/oncotargets-and-therapy-journal>

patient perspectives such as quality of life, adherence and satisfaction. The manuscript management system is completely online and includes a very quick and fair peer-review system, which is all easy to use. Visit <http://www.dovepress.com/testimonials.php> to read real quotes from published authors.

Dovepress